



Bi-directional thermoelastic analysis of pressurized thick cylindrical shell with nonlinear variable thickness

Fatemeh Ramezani ^a, Mohammad Zamani Nejad ^{a,*}, Mehdi Ghannad ^b

^a Department of Mechanical Engineering, Yasouj University, Yasouj, Iran

^b Mechanical Engineering Faculty, Shahrood University of Technology, Shahrood, Iran

Abstract

In this paper, a thermo-elastic analysis is presented to obtain stresses, displacements, and the thermal field in the axisymmetric clamped–clamped rotating thick cylindrical shell with nonlinear variable thickness. This shell is subjected to mechanical and thermal load in two dimensions. The governing equations are formulated as a set of non-homogeneous ordinary differential equations with variable coefficients. The system of partial differential equations is semi-analytically solved by using (MLM). The solution of equations is obtained by applying boundary conditions and ensuring continuity between the layers. The problem is also solved, using the finite element method (FEM). The obtained results of the disk form multi-layers method (MLM) are compared with those of FEM.

Keywords: Thermo-elastic; Thick cylinder; variable thickness; Multi-layer method (MLM); First-order shear deformation theory (FSDT); Bi-dimensional.

1. Introduction

Shells serve as prevalent structural components across numerous engineering applications, encompassing pressure vessels, submarine and ship hulls, aircraft wings and fuselages, pipes, rocket and missile exteriors, automobile tires, concrete roofs, chimneys, cooling towers, liquid storage tanks, and an array of other structures. Additionally, they exist in nature, manifested in entities such as eggs, leaves, inner ears, skulls, and geological formations. The art of crafting shell structures has been honed by humans over centuries [1]. A number of papers on shells are available (Fatehi and Nejad, [2]; Nejad et al. [3]; Mazarei et al. [4]; Nejad and Kashkoli [5]; Shahani and Kiarasi [6]; Nejad et al. [7]; Taghizade et al. [8]; Farajpour and Rastgoo [9]; Kashkoli et al. [10]; Nejad et al. [11]; Ebrahimi et al. [12]; Kashkoli et al. [13]; Dindarloo and Li [14]; Lamba [15]; Dehghan et al. [16]; Nejad and Fatehi [17]; Kashkoli et al. [18]; Delouei et al. [19]; Sofiyev and Fantuzzi [20]; Nejad et al. [21]; Zhang and She [22]; Ipek [23]; Kashkoli and Nejad [24, 25]). The practical and intriguing importance of shells in addressing temperature-related challenges has also captured the attention of researchers. Panferov [26] utilized the successive approximations method to derive a solution to the problem of thermal loading on an elastic truncated conical pipe that has a uniform thickness. Hongjun et al. [27] investigated the elasticity of heterogeneous thick-walled cylinders using the Lamé method to analyze cases involving linear and exponential changes in properties within the thick-walled cylinders. Arefi and Rahimi [28] investigated the thermoelastic behavior of a cylinder made of functionally graded material (FGM) when subjected to both mechanical and thermal loads. Nejad and Rahimi [29] studied deformations and stresses in FGM pressurized thick hollow cylinder based on closed form solutions for one-dimensional steady-state thermal stresses. Xin et al. [30] introduced a thermoelasticity solution for one-dimensional FG cylinders that is based on the constituents' volume fraction and accounts

* Corresponding author. Tel.: +98-7431005163; fax: +98-7431005000.
E-mail address: m_zamani@yu.ac.ir ; m.zamani.n@gmail.com

for both thermal and mechanical loads. Nejad et al. [31] presented on a consistent 3-D set of field equations developed by tensor analysis on an FGM thick shell with variable thickness. Yasinsky and Tokova [32] conducted a study on a one-dimensional temperature transient analysis and thermal stress analysis in a FG cylinder. Ghannad and Nejad [33] presented an elastic analysis of axisymmetric thick-walled cylinders with different boundary conditions at the two ends based on first-order shear deformation theory (FSDT) and the virtual work principle. Kang [34] studied thick-walled shells for arbitrary geometry and thickness variations using three-dimensional elasticity theory. The equations are derived using the continuum mechanics in curvilinear coordinates. Nejad et al. [35] developed an elastic solution to determine displacements and stresses in a thick truncated conical shell under uniform pressure. The solution employed the MLM. Ghannad et al. [36] studied displacements and stresses in pressurized thick cylindrical shells with variable thickness using the perturbation technique. Sundarasivarao and Ganesan [37] investigated a conical shell by using the finite element technique that was exposed to pressure. Mirsky and Hermann [38] studied the solution for thick cylindrical shells made of isotropic materials and uniform by utilizing the FSDT. Witt [39] demonstrated axisymmetric temperature distributions in conical shells using a differential equation. To solve this equation, Witt proposed an assumption that the temperature distribution could be a combination of hyperbolic and cubic functions. Eipakchi et al. [40] have analyzed thick-walled cone structures subjected to varying internal pressure. In this study, equations are derived using second-order shear deformation theory, and solutions are obtained through the perturbation theory approach. Ghannad and Nejad [41] investigated elastic solution of pressurized clamped-clamped thick cylindrical shells made of FGMs based on the FSDT. Jane and Wu [42] presented research on the problem of thermoelasticity using the curvilinear circular conical coordinate system. Ghannad et al. [43] obtained an elastic solution for truncated conical shells characterized by their significant thickness and uniform thickness distribution. Obata and Noda [44] analyzed steady one-dimensional thermal stresses in hollow cylindrical and spherical objects using perturbation technique. Ghannad et al. [45] analyzed the analytical solution of pressurized thick cylindrical shells with variable thickness based on the FSDT and using the asymptotic method (MAM) of the perturbation theory. Eipakchi [46] utilized a third-order shear deformation theory in conjunction with matched asymptotic expansion (MAE) from perturbation theory. This approach was applied to ascertain displacements and stresses within a thick conical shell. The shell's properties included homogeneity, isotropy, and axisymmetric, with non-uniform internal pressure leading to thickness variations. Kao et al. [47] provided an analytical solution for the buckling of cylindrical shell structures subjected to axial pressure. The symmetric and asymmetric axial loadings were solved using perturbation theory and Fourier series. Nejad et al. [48] presented semi-analytically of FG rotating thick hollow cylinder with variable thickness and clamped ends based on the FSDT using MLM. Civalek [49] utilized free vibration analysis in the of laminated conical shells. The author studied the cases of isotropic, orthotropic, and laminated materials and used the numerical solution of governing differential equations of motion based on transverse shear deformation theory to obtain the results. Nejad et al. [50] studied a mathematical solution that partially uses analysis and partially uses numerical methods to calculate the displacements and stresses in a cylindrical shell with varying thickness under a non-uniform pressure. They systematically examined how the primary factors of the problem affect displacement and stress levels. Ray et al. [51] conducted an analysis of heat conduction through conical shells with varying inner radii and thicknesses. Nejad et al. [52] studied a semi-analytical solution in rotating thick truncated conical shells made of FGMs under non-uniform pressure using FSDT and MLM. Jabbari et al. [53] employed a research on the thermoelastic analysis of a thick constant thickness truncated conical shell that rotates, and is exposed to a temperature gradient and non-uniform internal pressure. Jabbari et al. [54] utilized a thermo-elastic analysis of a rotating truncated conical shell subjected to temperature, internal pressure, and external pressure by using the FSDT and MLM. They derived a solution for the problem by reducing it to a reverse thermo-elasticity problem. Hamzah et al. [55] investigated a comprehensive study of the vibration characteristics of cylindrical shells under different ambient temperatures by using (FEM). Kashkoli [56] studied a thermomechanical solution for creep analysis of FG thick cylindrical pressure vessels with variable thickness using the FSDT and MLM. Gharooni et al. [57] studied an analytical solution in axisymmetric clamped-clamped thick cylindrical shells made of FGM Using the third-order shear deformation theory. Jabbari et al. [58] analyzed Thermo-elastic analysis in rotating truncated conical shells with varying thickness made of FGMs higher-order shear deformation theory and MLM. Lai et al. [59] introduced an analytical method for the analysis of thick-walled cylindrical shells with circumferential corrugations. The formulation and solution involve shear deformation theory, by using eigenvectors and Fourier series. Nejad et al. [60] presented thermo-elastic analysis in a FG thick shell of revolution with arbitrary curvature and variable thickness based on higher-order shear deformation theory. Aghaienezhad et al. [61] studied GDQ method to analyze the behavior of spherical and cylindrical shells subjected to external pressure. Ifayefunmi and Ruan [62] analyzed a computational finite element study on the instability behavior of cylinder shells under axial compressive load. Ariatapeh et al. [63] presented stress and deformation in thick-walled cylindrical pressure vessels/pipes made of Mooney-Rivlin hyperelastic materials. They presented their distributions, and evaluates the effects of various factors. Mannani et al. [64] studied the mechanical stress, static strain, and deformation of a cylindrical pressure vessel under mechanical

loads using higher-order sinusoidal shear deformation theory and thickness stretching formulation.

In this study, based on FSDT and multi-layer method, a thermo-elastic analysis presented for thick cylindrical shells with nonlinear variable thickness subjected mechanical and bi-directional thermal load.

2. Problem Formulation

Consider an axisymmetric, thick-walled cylindrical shell with an inner radius of r_i and a length of L . This shell with nonlinear variable thickness is subjected to uniform pressure, internal pressure P_i and external pressure P_o , while also rotating at a constant angular velocity ω (Fig. 1.). The displacement and temperature field in this shell is analyzed using the FSDT method. In the FSDT, sections initially straight and perpendicular to the mid-plane of the shell will remain straight after deformation, although they may not necessarily remain perfectly perpendicular. It is assumed that the shear strain remains constant across the thickness of the shell. The position of a typical point 'm' within the thick cylindrical shell element can be determined by R and z , as:

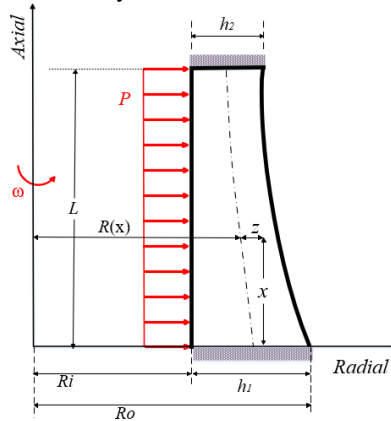


Fig. 1. Cross section of the rotating thick cylindrical pressure vessels with clamped-clamped ends.

$$\begin{cases} r = R(x) + z \\ 0 \leq x \leq L, \quad \frac{h}{2} \leq z \leq \frac{h}{2} \end{cases} \quad (1)$$

where z is the distance of a typical point from the middle surface and $R(x)$ represents the distance of the middle surface from the axial direction. Variable thickness h and $R(x)$ are as follow:

$$\begin{cases} R(x) = \frac{R_i + R_o}{2} \\ h = R_o - R_i \end{cases} \quad (2)$$

where R_o is tapering angle as:

$$R_o = R_i + h_1 - (h_1 - h_2) \left(\frac{x}{L} \right)^{0.5} \quad (3)$$

2.1. Thermal and mechanical field relation

In the FSDT, the general axisymmetric displacement field (U_x, U_z) and Temperature field (Θ_x, Θ_z) be defined in the following form

$$\begin{cases} \begin{Bmatrix} U_x \\ U_z \end{Bmatrix} = \begin{Bmatrix} u_0(x) \\ w_0(x) \end{Bmatrix} + \begin{Bmatrix} u_1(x) \\ w_1(x) \end{Bmatrix} z \\ \Theta(z, x) = T - T^* = \Theta^0(x) + z\Theta^1(x) = \Theta^0 + z\Theta^1 \end{cases} \quad (4)$$

Where $u_0(x)$ and $w_0(x)$ are the displacement components of the middle surface. Also, $u_1(x)$ and $w_1(x)$ are the functions used to determine the displacement field. T^* is assumed as the reference temperature and Θ^0, Θ^1 denote the temperature variations relative to a reference temperature, specifically representing the zero-order and first-order components, respectively.

In the thermal part due to the influence of $(\partial/\partial\theta)=0$, the temperature distribution function within the cylinder can

be expressed solely as a function of the radial coordinate (r) and the axial coordinate (x), therefore

$$T = T(r, x) \quad (5)$$

In the first-order temperature theory (FTT), the temperature field for this cylinder with varying thickness is expressed as follows [39, 65]:

$$\begin{aligned} T = T(z, x) &= T(0, x) + z \left. \frac{\partial T(z, x)}{\partial z} \right|_{z=0} + \frac{z^2}{2} \left. \frac{\partial^2 T(z, x)}{\partial z^2} \right|_{z=0} + \dots \\ &\approx T^0(x) + zT^1(x) = T^0 + zT^1 \end{aligned} \quad (6)$$

where, T^0 and T^1 are the zero-order and first-order components of temperature respectively, which are only a function of axial direction x . The strain-displacement relationships within a cylindrical coordinate system are as follows:

$$\begin{cases} \varepsilon_x = \frac{\partial U_x}{\partial x} = \frac{du_0}{dx} + \frac{du_1}{dx} z \\ \varepsilon_\theta = \frac{U_z}{r} = \frac{1}{R+z} (w_0 + w_1 z) \\ \varepsilon_z = \frac{\partial U_z}{\partial z} = w_1 \\ \gamma_{xz} = \frac{\partial U_x}{\partial z} + \frac{\partial U_z}{\partial x} = \left(u_1 + \frac{dw_0}{dx} \right) + \frac{dw_1}{dx} z \end{cases} \quad (7)$$

Also, the calculation of thermal strain and heat flux in an axisymmetric cylinder with varying thickness is performed as outlined below

$$\begin{Bmatrix} \varepsilon_z^t \\ \varepsilon_\theta^t \\ \varepsilon_x^t \\ \varepsilon_{zx}^t \end{Bmatrix} = \begin{Bmatrix} \alpha_{11} \\ \alpha_{22} \\ \alpha_{33} \\ \alpha_{13} \end{Bmatrix} \Theta \quad (8)$$

$$\begin{bmatrix} q_z \\ q_x \end{bmatrix} = \begin{bmatrix} K & 0 \\ 0 & K \end{bmatrix} \begin{bmatrix} e_z \\ e_x \end{bmatrix} \quad (9)$$

where $\varepsilon_z^t, \varepsilon_\theta^t, \varepsilon_x^t$ and ε_{zx}^t are the thermal strain. In addition, q_z and q_x are heat flux components in the radial (z) and axial (x) directions. Also, K is the thermal conduction coefficient. In Eq. (9), e_z, e_θ and e_x are thermal field components in the radial, circumferential, and axial directions which are defined as follows

$$\begin{cases} e_z = -\frac{\partial \Theta(x, z)}{\partial z} = -\Theta^1(x) \\ e_\theta = 0 \\ e_x = -\frac{\partial \Theta(x, z)}{\partial x} = -\frac{d\Theta^0(x)}{dx} - \frac{d\Theta^1(x)}{dx} z \end{cases} \quad (10)$$

Taking into account the impact of thermal strain in homogeneous and isotropic materials, the stress-strain relations, or constitutive equations, are as follows:

$$\begin{bmatrix} \sigma_z \\ \sigma_\theta \\ \sigma_x \\ \tau_{zx} \end{bmatrix} = \frac{E}{(1-2\nu)(1+\nu)} \begin{bmatrix} 1-\nu & \nu & \nu & 0 \\ \nu & 1-\nu & \nu & 0 \\ \nu & \nu & 1-\nu & 0 \\ 0 & 0 & 0 & \frac{(1-2\nu)}{2} \end{bmatrix} \begin{bmatrix} \varepsilon_z \\ \varepsilon_\theta \\ \varepsilon_x \\ \gamma_{zx} \end{bmatrix} - \frac{E}{(1-2\nu)} \begin{bmatrix} \alpha \\ \alpha \\ \alpha \\ 0 \end{bmatrix} T \quad (11)$$

Here, $\sigma_z, \sigma_\theta, \sigma_x, \tau_{zx}$ and $\varepsilon_z, \varepsilon_\theta, \varepsilon_x, \gamma_{zx}$ are the stresses and strains in the axial (x), circumferential (θ) and radial (z) directions, respectively. Furthermore, ν, E, α and T are Poisson's ratio, modulus of elasticity, the coefficient of thermal expansion and temperature gradient, respectively.

The normal forces ($N_z^{m,t}, N_\theta^{m,t}, N_x^{m,t}$), bending moments ($M_z^{m,t}, M_\theta^{m,t}, M_x^{m,t}$), shear force (Q_x), and the torsional moment (M_{zx}) in terms of mechanical(index m) and thermal (index t) stress resultants are:

$$\begin{cases} N_z^m \\ N_\theta^m \\ N_x^m \end{cases} = \int_{-h/2}^{h/2} \begin{cases} \sigma_z(1+\frac{z}{R}) \\ \sigma_\theta \\ \sigma_x(1+\frac{z}{R}) \end{cases} dz$$

$$\begin{cases} M_\theta^m \\ M_x^m \end{cases} = \int_{-h/2}^{h/2} \begin{cases} \sigma_\theta \\ \sigma_x(1+\frac{z}{R}) \end{cases} z dz$$

$$\begin{cases} Q_x^m \\ M_{zx}^m \end{cases} = k \int_{-h/2}^{h/2} \begin{cases} 1 \\ z \end{cases} \tau_{zx} \left(1+\frac{z}{R}\right) dz$$

$$\begin{cases} N_z^t \\ N_x^t \end{cases} = \int_{-h/2}^{h/2} \begin{cases} h_z \\ h_x \end{cases} \left(1+\frac{z}{R}\right) dz$$

$$M_z^t = \int_{-h/2}^{h/2} h_x \left(1+\frac{z}{R}\right) z dz \tag{12}$$

In this paper, k represents a correction factor that is introduced into the shear stress term. In the static state, for cylindrical shells $k = 5/6$ [66].

2.2. Equilibrium Equations

In accordance with the principle of virtual work, the changes in strain energy are equal to the changes in external work done. The total energy Π can be represented as $\Pi = U - W$ where U is the total strain energy of the body and W is the total external work done on the body by the total specified external forces. By substituting strain energy and the work of external forces, we have

$$\delta U = \int_0^L \int_0^{2\pi} \int_{-h/2}^{h/2} \frac{1}{2} \begin{pmatrix} \sigma_z \delta \epsilon_z + \sigma_\theta \delta \epsilon_\theta + \sigma_x \delta \epsilon_x \\ + \tau_{zx} \delta \gamma_{zx} - h_x \delta e_x - h_z \delta e_z \end{pmatrix} (R+z) dz d\theta dx \tag{13}$$

$$\delta W = \int_0^L \int_0^{2\pi} \left(P \delta U_z - H_i \delta \Theta \right) \left(R - \frac{h}{2} \right) + H_o \delta \Theta \left(R + \frac{h}{2} \right) dx d\theta \tag{14}$$

By substituting Eqs. (13,14) into $\Pi = U - W$ and applying the calculus of variation and the virtual work principle with respect to Eq. (12), we derive the governing equations as follows:

$$\begin{cases} -\frac{d}{dx} \left(RN_x^m \right) = 0 \\ RQ_x^m - \frac{d}{dx} \left(RM_x^m \right) = 0 \\ RN_z^m - \frac{d}{dx} \left(RM_{zx}^m \right) + M_\theta^m = -P \frac{h}{2} \left(R - \frac{h}{2} \right) + \frac{\rho \omega^2}{6} Rh^3 \\ N_\theta^m - \frac{d}{dx} \left(RQ_\theta^m \right) = P \left(R - \frac{h}{2} \right) + \frac{\rho \omega^2}{6} \frac{h}{2} \left(12R^2 + h^2 \right) \\ -\frac{d}{dx} \left(RN_x^t \right) = H_o \left(R + \frac{h}{2} \right) - H_i \left(R - \frac{h}{2} \right) \\ RN_z^t - \frac{d}{dx} \left(RM_x^t \right) = H_i \frac{h}{2} \left(R - \frac{h}{2} \right) + H_o \left(R + \frac{h}{2} \right) \end{cases} \tag{15}$$

Additionally, the boundary conditions are as follows:

$$\frac{d}{dx} \left(\begin{array}{l} RN_x^m \delta u + RM_x^m \delta \varphi + RQ_x^m \delta w + RM_{zx}^m \delta \psi \\ + RN_x^t \delta \Theta^0(x) + RM_x^t \delta \Theta^1(x) \end{array} \right) = 0 \quad (16)$$

The number of thermal and mechanical resultants does not match the number of equations specified in Eq. (15). Therefore, to solve the set of differential equations Eq. (16), it is necessary to express thermal and mechanical quantities in terms of the components of the temperature and displacement fields. Eq. (16) defines the boundary conditions that must be satisfied at the two ends of the cylinder. By substituting Eq. (12) into Eq. (15), the set of differential equations (Eq. (15)) can be rewritten as follows

$$[A_1] \frac{d^2}{dx^2} \{\bar{y}\} + [A_2] \frac{d}{dx} \{\bar{y}\} + [A_3] \{\bar{y}\} = [F] \quad (17)$$

$$\{\bar{y}\} = \left\{ \frac{du_0}{dx}, u, w_0, w_1, \frac{d\Theta^0}{dx}, \Theta^1 \right\} \quad (18)$$

where $[A_1]_{6 \times 6}$, $[A_2]_{6 \times 6}$, $[A_3]_{6 \times 6}$ are the coefficients matrices, and F is the force vector, as:

$$[A_1] = \begin{bmatrix} 0 & 0 & 0 \\ 0 & -\frac{E(1-\nu)}{(1-2\nu)(1+\nu)} R \frac{h^3}{12} & 0 \\ 0 & 0 & -k \frac{E}{2(1+\nu)} Rh \\ 0 & 0 & -k \frac{E}{2(1+\nu)} \frac{h^3}{12} \\ 0 & 0 & 0 \\ 0 & 0 & 0 \\ 0 & 0 & 0 \\ 0 & 0 & 0 \\ -k \frac{E}{2(1+\nu)} \frac{h^3}{12} & 0 & 0 \\ -k \frac{E}{2(1+\nu)} R \frac{h^3}{12} & 0 & 0 \\ 0 & 0 & 0 \\ 0 & R \int_{-h/2}^{h/2} Kz dz & R \int_{-h/2}^{h/2} Kz^3 dz \end{bmatrix} \quad (19)$$

$$[A_2] = \begin{bmatrix} 0 & \frac{E(1-\nu)}{(1-2\nu)(1+\nu)} \frac{h^3}{12} & 0 \\ -\frac{E(1-\nu)}{(1-2\nu)(1+\nu)} \frac{h^3}{12} & -\frac{(1-\nu)}{(1-2\nu)(1+\nu)} \frac{h^2}{12} \left(3R \frac{dh}{dx} \right) & k \frac{E}{2(1+\nu)} Rh \\ 0 & -k \frac{E}{2(1+\nu)} Rh & -\frac{k}{2(1+\nu)} \left(RE \frac{dh}{dx} \right) \\ 0 & \frac{E}{(1+\nu)} \frac{h^3}{12} \left(\frac{2\nu}{(1-2\nu)} - \frac{k}{2} \right) & -\frac{kE}{2(1+\nu)} \frac{h^2}{4} \frac{dh}{dx} \\ 0 & 0 & 0 \\ 0 & 0 & 0 \end{bmatrix}$$

$$\begin{bmatrix} 0 & 0 & 0 \\ \frac{E}{(1+\nu)} \frac{h^3}{12} \left(\frac{k}{2} - \frac{\nu}{(1-2\nu)} \right) & \frac{E(1+\nu)}{(1-2\nu)(1+\nu)} \frac{h^3}{12} \alpha & \frac{E(1+\nu)}{(1-2\nu)(1+\nu)} R \frac{h^3}{12} \alpha \\ -\frac{kE}{2(1+\nu)} \frac{h^2}{4} \frac{dh}{dx} & 0 & 0 \\ -\frac{k}{2(1+\nu)} \frac{h^2}{12} \left(3RE \frac{dh}{dx} \right) & 0 & 0 \\ 0 & 0 & 0 \\ 0 & 0 & 0 \end{bmatrix} \tag{20}$$

$$[A_3] = \begin{bmatrix} \frac{E(1-\nu)}{(1-2\nu)(1+\nu)} Rh & 0 & \frac{Ev}{(1-2\nu)(1+\nu)} h \\ -\frac{E(1-\nu)}{(1-2\nu)(1+\nu)} \frac{h^2}{4} \frac{dh}{dx} & k \frac{E}{2(1+\nu)} Rh & 0 \\ \frac{Ev}{(1-2\nu)(1+\nu)} h & -\frac{kE}{2(1+\nu)} \left(R \frac{dh}{dx} \right) & \frac{E(1-\nu)}{(1-2\nu)(1+\nu)} \ln \left(\frac{R+\frac{h}{2}}{R-\frac{h}{2}} \right) \\ \frac{Ev}{(1-2\nu)(1+\nu)} Rh & -\frac{kE}{2(1+\nu)} \frac{h^2}{4} \frac{dh}{dx} & \frac{E}{(1-2\nu)(1+\nu)} \left(h - (1-\nu) R \ln \left(\frac{R+\frac{h}{2}}{R-\frac{h}{2}} \right) \right) \\ 0 & 0 & 0 \\ 0 & 0 & 0 \end{bmatrix}$$

$$\begin{bmatrix} \frac{Ev}{(1-2\nu)(1+\nu)} Rh & -\frac{E(1+\nu)}{(1-2\nu)(1+\nu)} Rh\alpha & -\frac{E(1+\nu)}{(1-2\nu)(1+\nu)} \frac{h^3}{12} \alpha \\ \frac{Ev}{(1-2\nu)(1+\nu)} \frac{h^2}{2} \frac{dh}{dx} & \frac{(1+\nu)}{(1-2\nu)(1+\nu)} \frac{h^2}{12} \left(3\alpha E \frac{dh}{dx} \right) & \frac{(1+\nu)}{(1-2\nu)(1+\nu)} \frac{h^2}{12} \left(3\alpha ER \frac{dh}{dx} \right) \\ -\frac{E}{(1-2\nu)(1+\nu)} \left(h - (1-\nu) R \ln \left(\frac{R+\frac{h}{2}}{R-\frac{h}{2}} \right) \right) & -\frac{E(1+\nu)}{(1-2\nu)(1+\nu)} h\alpha & 0 \\ \frac{E(1-\nu)}{(1-2\nu)(1+\nu)} R^3 \ln \left(\frac{R+\frac{h}{2}}{R-\frac{h}{2}} \right) & -\frac{E(1+\nu)}{(1-2\nu)(1+\nu)} Rh\alpha & -\frac{E(1+\nu)}{(1-2\nu)(1+\nu)} \frac{h^3}{6} \alpha \\ 0 & -R \int_{-h/2}^{h/2} K dz & -\int_{-h/2}^{h/2} K z^2 dz \\ 0 & 0 & -\int_{-h/2}^{h/2} K (R+z) dz \end{bmatrix} \tag{21}$$

$$[F] = \begin{Bmatrix} C_1 \\ 0 \\ P \frac{h}{2} \left(R - \frac{h}{2} \right) + \frac{\rho \omega^2}{6} R h^3 \\ -P \left(R - \frac{h}{2} \right) + \frac{\rho \omega^2}{6} \frac{h}{2} (12R^2 + h^2) \\ \left[H_o \left(R - \frac{h}{2} \right) - H_i \left(R + \frac{h}{2} \right) \right] x + C_2 \\ \frac{h}{2} \left[H_i \left(R - \frac{h}{2} \right) + H_o \left(R + \frac{h}{2} \right) \right] \end{Bmatrix} \quad (22)$$

3. Thermo-Elastic Solution

3.1. Multi-Layered Method (MLM)

In the Method of Layering (MLM), a homogeneous cylinder subjected to non-uniform pressure is divided into disc-shaped layers with a small thickness $h^{[k]}$. Under these assumptions, the set of nonhomogeneous linear differential equations is transformed into a set of nonhomogeneous differential equations with constant coefficients using the MLM. The equations for each homogeneous disc with a small thickness are obtained as follows

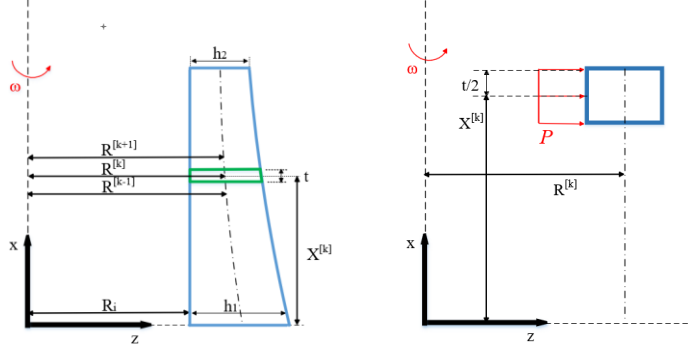


Fig. 2. Division of cylindrical shell with variable thickness to homogenous disks with constant thickness.

As a result, the governing equations are transformed into a non-homogeneous set of differential equations featuring constant coefficients. $x^{[k]}$ and $R^{[k]}$ are length and radius of middle of disks. The modulus of elasticity and Poisson's ratio of disks are assumed be constant. The length of middle of an arbitrary disk (Fig. 2.) is as follows

$$\begin{cases} R^{[k]}(x) = \frac{R_i^{[k]} + R_o^{[k]}}{2} \\ h^{[k]} = R_o^{[k]} - R_i^{[k]} \end{cases} \quad (23)$$

where

$$R_o^{[k]} = R_i + h_1 - (h_1 - h_2) \left(\frac{x^{[k]}}{L} \right) \quad (24)$$

Thus

$$\left(\frac{dh}{dx} \right)^{[k]} = 2 \left(\frac{dR}{dx} \right)^{[k]} = \left(\left(\frac{dR_o}{dx} \right)^{0.5} \right)^{[k]} \quad (25)$$

Poisson's ratio of disks is assumed to be constant. The governing equations for each homogenous disk are derived as follow

$$[A_1]^{[k]} \frac{d^2}{dx^2} \{\bar{y}\}^{[k]} + [A_2]^{[k]} \frac{d}{dx} \{\bar{y}\}^{[k]} + [A_3]^{[k]} \{\bar{y}\}^{[k]} = [F]^{[k]} \quad (26)$$

$$\{\bar{y}\}^{[k]} = \left\{ \left(\frac{du_0}{dx} \right)^{[k]}, u_1^{[k]}, w_0^{[k]}, w_1^{[k]}, \left(\frac{d\theta^0}{dx} \right)^{[k]}, \theta^{[k]} \right\}^T \tag{27}$$

$[A_1]_{6 \times 6}^{[k]}$ The coefficients matrices and $\{F\}_{6 \times 6}^{[k]}$ force vector are as follows:

$$[A_1] = \begin{bmatrix} 0 & 0 & 0 & 0 & 0 & 0 \\ 0 & -\frac{E(1-\nu)}{(1-2\nu)(1+\nu)} R^{[k]} \frac{h^{[k]3}}{12} & 0 & 0 & 0 & 0 \\ 0 & 0 & -k \frac{E}{2(1+\nu)} R^{[k]} h^{[k]} & 0 & 0 & 0 \\ 0 & 0 & -k \frac{E}{2(1+\nu)} \frac{h^{[k]3}}{12} & 0 & 0 & 0 \\ 0 & 0 & 0 & 0 & 0 & 0 \\ 0 & 0 & 0 & 0 & 0 & 0 \\ -k \frac{E}{2(1+\nu)} \frac{h^{[k]3}}{12} & 0 & 0 & 0 & 0 & 0 \\ -k \frac{E}{2(1+\nu)} R^{[k]} \frac{h^{[k]3}}{12} & 0 & 0 & 0 & 0 & 0 \\ 0 & 0 & 0 & 0 & 0 & 0 \\ 0 & R^{[k]} \int_{-h^{[k]}/2}^{h^{[k]}/2} K_z dz & h^{[k]}/2 \int_{-h^{[k]}/2}^{h^{[k]}/2} K_z dz & 0 & 0 & 0 \\ & -h^{[k]}/2 \int_{-h^{[k]}/2}^{h^{[k]}/2} K_z dz & -h^{[k]}/2 \int_{-h^{[k]}/2}^{h^{[k]}/2} K_z dz & 0 & 0 & 0 \end{bmatrix} \tag{28}$$

$$[A_2] = \begin{bmatrix} 0 & \frac{E(1-\nu)}{(1-2\nu)(1+\nu)} \frac{h^{[k]3}}{12} & 0 & 0 & 0 & 0 \\ -\frac{E(1-\nu)}{(1-2\nu)(1+\nu)} \frac{h^{[k]3}}{12} & -\frac{(1-\nu)}{(1-2\nu)(1+\nu)} \frac{h^{[k]2}}{12} \left(3R^{[k]} \frac{dh^{[k]}}{dx} \right) & k \frac{E}{2(1+\nu)} R^{[k]} h^{[k]} & 0 & 0 & 0 \\ 0 & -k \frac{E}{2(1+\nu)} R^{[k]} h^{[k]} & -\frac{k}{2(1+\nu)} \left(R^{[k]} \int_E \frac{dh^{[k]}}{dx} \right) & 0 & 0 & 0 \\ 0 & \frac{E}{(1+\nu)} \frac{h^{[k]3}}{12} \left(\frac{2\nu}{(1-2\nu)} - \frac{k}{2} \right) & -\frac{kE}{2(1+\nu)} \frac{h^{[k]2}}{4} \frac{dh^{[k]}}{dx} & 0 & 0 & 0 \\ 0 & 0 & 0 & 0 & 0 & 0 \\ 0 & 0 & 0 & 0 & 0 & 0 \\ \frac{E}{(1+\nu)} \frac{h^{[k]3}}{12} \left(\frac{k}{2} - \frac{\nu}{(1-2\nu)} \right) & \frac{E(1+\nu)}{(1-2\nu)(1+\nu)} \frac{h^{[k]3}}{12} \alpha & \frac{E(1+\nu)}{(1-2\nu)(1+\nu)} R^{[k]} \frac{h^{[k]3}}{12} \alpha & 0 & 0 & 0 \\ -\frac{kE}{2(1+\nu)} \frac{h^{[k]2}}{4} \frac{dh^{[k]}}{dx} & 0 & 0 & 0 & 0 & 0 \\ -\frac{k}{2(1+\nu)} \frac{h^{[k]2}}{12} \left(3R^{[k]} \int_E \frac{dh^{[k]}}{dx} \right) & 0 & 0 & 0 & 0 & 0 \\ 0 & 0 & 0 & 0 & 0 & 0 \\ 0 & 0 & 0 & 0 & 0 & 0 \end{bmatrix} \tag{29}$$

$$\left[A_3 \right] = \begin{bmatrix} \frac{E(1-\nu)}{(1-2\nu)(1+\nu)} R^{[k]}_h [k] & 0 & \frac{E\nu}{(1-2\nu)(1+\nu)} h^{[k]} \\ \frac{E(1-\nu)}{(1-2\nu)(1+\nu)} \frac{h^{[k]2}}{4} \frac{dh^{[k]}}{dx} & k \frac{E}{2(1+\nu)} R^{[k]}_h [k] & 0 \\ \frac{E\nu}{(1-2\nu)(1+\nu)} h^{[k]} & -\frac{kE}{2(1+\nu)} \left(R \frac{dh^{[k]}}{dx} \right) & \frac{E(1-\nu)}{(1-2\nu)(1+\nu)} \ln \left(\frac{R + \frac{h^{[k]}}{2}}{R - \frac{h^{[k]}}{2}} \right) \\ \frac{E\nu}{(1-2\nu)(1+\nu)} R^{[k]}_h [k] & -\frac{kE}{2(1+\nu)} \frac{h^{[k]2}}{4} \frac{dh^{[k]}}{dx} & \frac{E}{(1-2\nu)(1+\nu)} \left(h^{[k]} - (1-\nu) R^{[k]} \ln \left(\frac{R^{[k]} + \frac{h^{[k]}}{2}}{R^{[k]} - \frac{h^{[k]}}{2}} \right) \right) \\ 0 & 0 & 0 \\ 0 & 0 & 0 \\ \frac{E\nu}{(1-2\nu)(1+\nu)} R^{[k]}_h [k] & -\frac{E(1+\nu)}{(1-2\nu)(1+\nu)} R^{[k]}_h [k] \alpha^{[k]} & -\frac{E(1+\nu)}{(1-2\nu)(1+\nu)} \frac{h^{[k]3}}{12} \alpha^{[k]} \\ \frac{E\nu}{(1-2\nu)(1+\nu)} \frac{h^{[k]2}}{2} \frac{dh^{[k]}}{dx} & \frac{(1+\nu)}{(1-2\nu)(1+\nu)} \frac{h^{[k]2}}{12} \left(3\alpha^{[k]} E \frac{dh^{[k]}}{dx} \right) & \frac{(1+\nu)}{(1-2\nu)(1+\nu)} \frac{h^{[k]2}}{12} \left(3\alpha^{[k]} E R^{[k]} \frac{dh^{[k]}}{dx} \right) \\ -\frac{E}{(1-2\nu)(1+\nu)} \left(h^{[k]} - (1-\nu) R^{[k]} \ln \left(\frac{R^{[k]} + \frac{h^{[k]}}{2}}{R - \frac{h^{[k]}}{2}} \right) \right) & -\frac{E(1+\nu)}{(1-2\nu)(1+\nu)} h^{[k]} \alpha^{[k]} & 0 \\ \frac{E(1-\nu)}{(1-2\nu)(1+\nu)} R^{[k]3} \ln \left(\frac{R^{[k]} + \frac{h^{[k]}}{2}}{R^{[k]} - \frac{h^{[k]}}{2}} \right) & -\frac{E(1+\nu)}{(1-2\nu)(1+\nu)} R^{[k]}_h [k] \alpha^{[k]} & -\frac{E(1+\nu)}{(1-2\nu)(1+\nu)} \frac{h^{[k]3}}{6} \alpha^{[k]} \\ 0 & -R^{[k]} \int_{-h^{[k]}/2}^{h^{[k]}/2} K dz & -\int_{-h^{[k]}/2}^{h^{[k]}/2} K z^2 dz \\ 0 & 0 & -\int_{-h^{[k]}/2}^{h^{[k]}/2} K(R+z) dz \end{bmatrix} \tag{30}$$

$$\left[F \right] = \left\{ \begin{array}{l} C_1 \\ 0 \\ P \frac{h^{[k]}}{2} \left(R^{[k]} - \frac{h^{[k]}}{2} \right) + \frac{\rho\omega^2}{6} R^{[k]}_h [k]^3 \\ -P \left(R^{[k]} - \frac{h^{[k]}}{2} \right) + \frac{\rho\omega^2}{6} \frac{h^{[k]}}{2} \left(12R^{[k]2} + h^{[k]2} \right) \\ \left[H_o \left(R^{[k]} - \frac{h^{[k]}}{2} \right) - H_i \left(R^{[k]} + \frac{h^{[k]}}{2} \right) \right] x + C_2 \\ \frac{h^{[k]}}{2} \left[H_i \left(R^{[k]} - \frac{h^{[k]}}{2} \right) + H_o \left(R^{[k]} + \frac{h^{[k]}}{2} \right) \right] \end{array} \right\} \tag{31}$$

Defining the differential operator $P(D)$, Eq. (3) is written as:

$$\begin{cases} [P(D)]^{[k]} = [B_1]^{[k]} D^2 + [B_2]^{[k]} D + [B_3]^{[k]} \\ D^2 = \frac{d^2}{dx^2}, D = \frac{d}{dx} \end{cases} \quad (32)$$

Thus

$$[P(D)]^{[k]} \{y\}^{[k]} = \{F\}^{[k]} \quad (33)$$

The above differential equation represents the complete solution, which includes the general solution for the homogeneous case. The homogeneous case is as follows:

$$\{y\}^{[k]} = \{y\}_h^{[k]} + \{y\}_p^{[k]} \quad (34)$$

Therefore, the complete solution for both the thermal and mechanical aspects is expressed as follows:

$$\begin{Bmatrix} U_x^{[k]} \\ U_z^{[k]} \\ \theta^{[k]} \end{Bmatrix} = \begin{Bmatrix} U_x^{[k]} \\ U_z^{[k]} \\ \theta^{[k]} \end{Bmatrix}_h + \begin{Bmatrix} U_x^{[k]} \\ U_z^{[k]} \\ \theta^{[k]} \end{Bmatrix}_p \quad (35)$$

In a general state, the thermoelastic solution for each disk comprises 12 unknown values denoted as $C_i^{[k]}, C_j^{\tau[k]}$ and an eighth-order polynomial. This polynomial consists of a sixth-order polynomial pertaining to displacement and a second-order polynomial related to thermal effects. The determination of these $C_i^{[k]}, C_j^{\tau[k]}$ values is finalized by applying the appropriate boundary and continuity conditions to complete the result of the determinant mentioned above.

4. Boundary and Continuity Conditions

In this problem, the boundary conditions for the clamped-clamped cylindrical shell subjected to temperature are as follows:

$$\begin{Bmatrix} u_0, u_1 \\ w_0, w_1 \\ \Theta^0 \\ \Theta^1 \end{Bmatrix}_{x=0} = \begin{Bmatrix} u_0, u_1 \\ w_0, w_1 \\ \Theta^0 \\ \Theta^1 \end{Bmatrix}_{x=L} = \begin{Bmatrix} 0 \\ 0 \\ T - T_{ref} \\ 0 \end{Bmatrix} \quad (36)$$

In disk form multi-layers method (MLM), at the boundary between two layers, forces, stresses, and displacements remain continuous due to the overall continuity and homogeneity of the cylinder. The continuity conditions are as follows:

$$\begin{Bmatrix} U_x^{[k-1]}(x, z) \\ U_z^{[k-1]}(x, z) \end{Bmatrix}_{x=x^{[k-1]} + \frac{t}{2}} = \begin{Bmatrix} U_x^{[k]}(x, z) \\ U_z^{[k]}(x, z) \end{Bmatrix}_{x=x^{[k]} - \frac{t}{2}} \quad (37)$$

$$\begin{Bmatrix} U_x^{[k]}(x, z) \\ U_z^{[k]}(x, z) \end{Bmatrix}_{x=x^{[k]} + \frac{t}{2}} = \begin{Bmatrix} U_x^{[k+1]}(x, z) \\ U_z^{[k+1]}(x, z) \end{Bmatrix}_{x=x^{[k+1]} - \frac{t}{2}} \quad (38)$$

And

$$\begin{Bmatrix} \frac{dU_x^{[k-1]}(x, z)}{dx} \\ \frac{dU_z^{[k-1]}(x, z)}{dx} \end{Bmatrix}_{x=x^{[k-1]} + \frac{t}{2}} = \begin{Bmatrix} \frac{dU_x^{[k]}(x, z)}{dx} \\ \frac{dU_z^{[k]}(x, z)}{dx} \end{Bmatrix}_{x=x^{[k]} - \frac{t}{2}} \quad (39)$$

$$\left\{ \begin{array}{l} \frac{dU_x^{[k]}(x,z)}{dx} \\ \frac{dU_z^{[k]}(x,z)}{dx} \end{array} \right\}_{x=x^{[k]}+\frac{t}{2}} = \left\{ \begin{array}{l} \frac{dU_x^{[k+1]}(x,z)}{dx} \\ \frac{dU_z^{[k+1]}(x,z)}{dx} \end{array} \right\}_{x=x^{[k+1]}-\frac{t}{2}} \tag{40}$$

According to the continuity conditions, in terms of z, T , 12 equations are obtained. In general, if the shell is divided into n disk layers, $12(n-1)$ equations are obtained. Utilizing the 12 equations of boundary condition, 12n equations are obtained. The solution of these equations yields $12n$ unknown constants.

5. Results and discussion

The solution described in the preceding section is applicable to a cylindrical shell with nonlinear variable thickness h , $h_1=40$ mm, $h_2=20$ mm, $R_1=100$ mm and $L=1000$ mm will be considered subjected to uniform pressure. The key parameters and conditions for this problem are as: $E=117$ GPa, $\nu=0.3$, $\alpha=22(10^{-6})$ 1/°C and $\kappa=391$ W/m°C. Mechanical loading is applied in the form of uniform internal pressure with values of $P=80$ MPa, and the cylinder rotates with $\omega=150$ rad/s. Thermal loading is in the form of internal heat flux of $H_i=150$ W/m² and applied temperature at the heads of the shell with values of $T_1=50$ °C and $T_2=50$ °C. The cylindrical shell is subject to clamped-clamped boundary conditions. Displacement and stresses are normalized by dividing them by the internal radii and the internal pressure, respectively. The material properties of the constituent are evaluated at the reference temperature $T^*=25$ °C.

The displacement distributions obtained through MLM are compared with those derived from FEM solutions, and these comparisons are graphically presented in Fig. 3. The number of disk layers is considered to be 80 for achieving convergence in this context. Increasing the number of layers beyond 80 in this study has no effect on the output results. Notably, the results demonstrate a strong alignment with validated FEM outcomes. Based on the observations obtained from the figure below, the radial displacement of points distant from the border increases along the length, while, under the same conditions, the radial displacement decreases from the inner layer to the outer layer at a specific point.

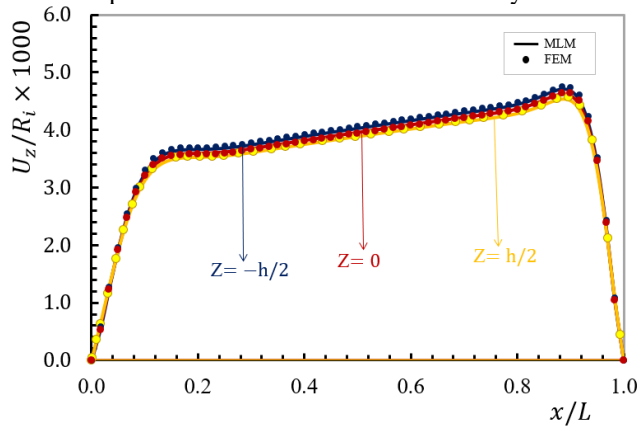


Fig. 3. Normalized radial displacement distribution in different layers ($\omega=500$ rad/s)

Fig. 4. shows the values of shear stress in three specific layers in the longitudinal direction. Based on the observations, the values of shear stress in the longitudinal direction can be ignored.

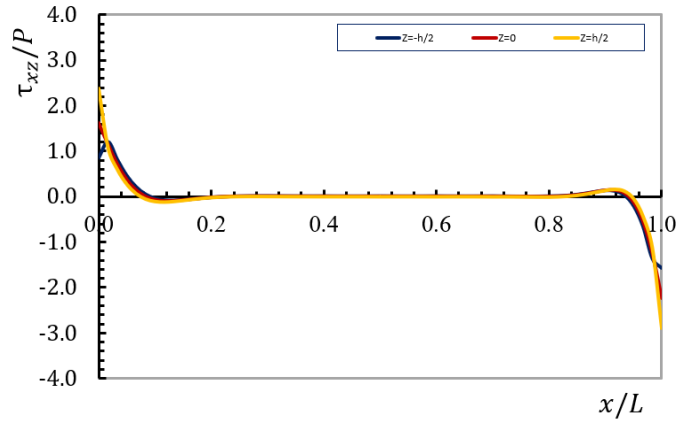


Fig. 4 Normalized shear stress distribution in different layers ($\omega = 500$ rad/s)

In Fig. 5, the changes in circumferential stress are depicted in terms of the cylinder's length. Across all three investigated layers, the circumferential stresses are tensile. At a specific point of interest, the circumferential stress has decreased from the inner layer to the outer layer. Furthermore, it's worth noting that the circumferential stress exhibits an increase in the longitudinal direction.

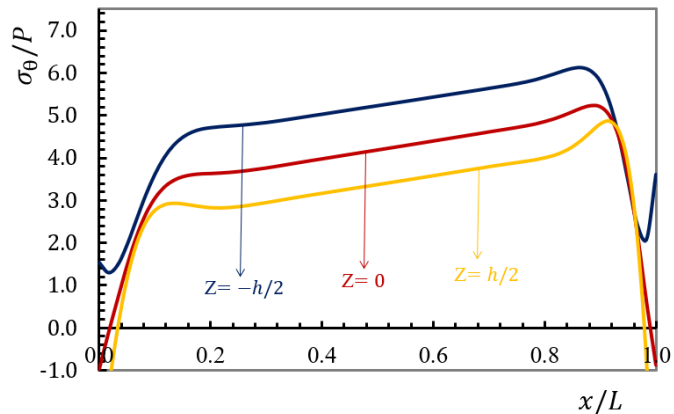


Fig. 5. Normalized circumferential stress distribution in different layers ($\omega = 500$ rad/s)

In Fig. 6, von Mises stress is utilized to represent the equivalent stress in the longitudinal direction. von Mises stress increases in points far from the boundary in the longitudinal direction and gives tensile values. Furthermore, these equivalent stress values decrease from the inner layer to the outer layer.

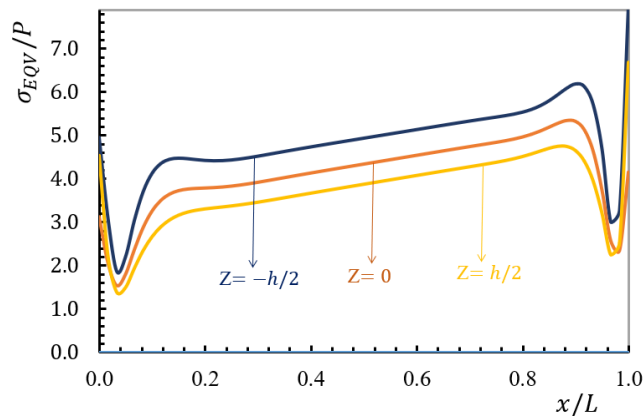


Fig. 6. Normalized equivalent stress distribution in different layers ($\omega = 500$ rad/s)

In Figs. 7 - 10, the effects of angular velocity on displacement and stresses have been investigated. As shown in the Fig. 7, In the investigation of radial displacement in the middle layer, it was observed that the amount of radial displacement increased with the increase in ω for points far from the boundary. This change in the longitudinal

direction is also incremental. Furthermore, the shape of the displacement profiles in the figure below remained consistent when compared to the displacement profile in Fig. 3.

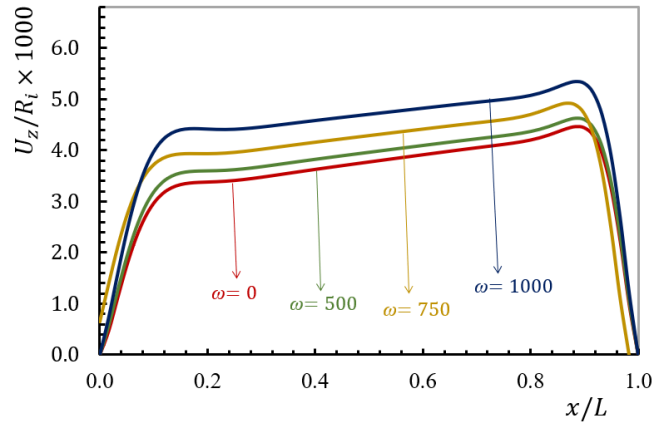


Fig. 7. Normalized radial displacement distribution subjected to different angular velocity ($h = 0$)

In Fig. 8, the shear stress distribution along the length of the cylinder is illustrated at different angular velocities. As indicated in the figure, like in Fig. 4, it is apparent that shear stress can be safely ignored in all layers when positioned far from the boundary. Additionally, the effect of angular velocity on shear stress is negligible.

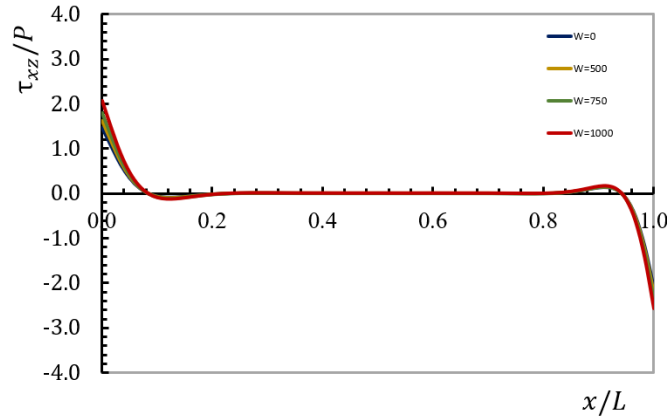


Fig. 8. Normalized shear stress distribution subjected to different angular velocity ($h = 0$)

In Fig. 9, the investigated circumferential stress behavior at different angular velocities is similar to Fig. 5. As the angular velocity increases, the circumferential stress increases and this stress remains tensile.

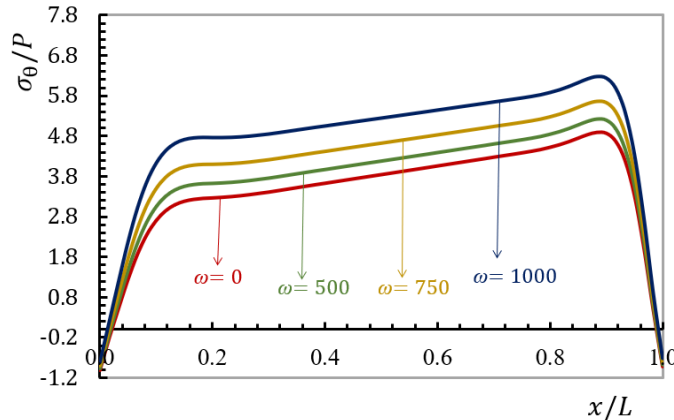


Fig. 9. Normalized circumferential stress distribution subjected to different angular velocity ($h = 0$)

In Fig. 10, the equivalent stress at different angular velocities in the middle layer has been investigated. An increase in angular velocity leads to an increase in equivalent stress. In addition, the equivalent stress is increasing in the longitudinal direction.

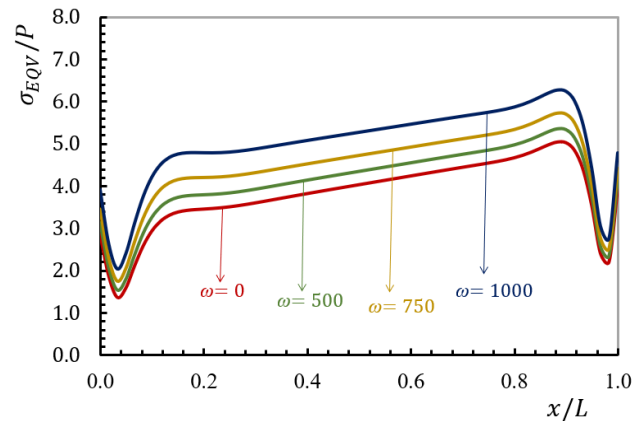


Fig. 10. Normalized equivalent stress distribution subjected to different angular velocity ($h=0$)

6. Conclusions

In this article, the governing equations in a cylinder with a nonlinear variable thickness under mechanical and bi-directional thermal loading have been investigated. In this cylinder, the relations have been obtained using the theory of first-order shear deformation and the MLM. Temperature has been investigated in two directions. The results of stresses and displacements have been compared with the finite element method and the results have shown good agreement. To calculate the equivalent stress, the von Mises stress has been used. In the outputs of this study, the effect of angular velocity has been investigated under the boundary conditions of the clamp-clamp.

The method of MLM that utilizes multilayered discs shows promise as an alternative for assessing thick-walled shells. With this approach, it becomes easier to solve problems involving shells of varying shapes, diverse loading conditions, different boundary constraints, and even fluctuating pressures. This stands in contrast to existing analytical methods, which encounter difficulties because of their complex mathematical formulations. The described technique is especially suited for determining radial stress, circumferential stress, shear stress, and radial displacement.

References

- [1] C. Wang, J. N. Reddy, K. Lee, 2000, *Shear deformable beams and plates: Relationships with classical solutions*, Elsevier.
- [2] P. Fatehi, M. Z. Nejad, Effects of material gradients on onset of yield in FGM rotating thick cylindrical shells, *International Journal of Applied Mechanics*, Vol. 6, No. 4, pp. 1450038, 2014.
- [3] M. Z. Nejad, A. Rastgoo, A. Hadi, Exact elasto-plastic analysis of rotating disks made of functionally graded materials, *International Journal of Engineering Science*, Vol. 85, pp. 47-57, 2014.
- [4] Z. Mazarei, M. Z. Nejad, A. Hadi, Thermo-elasto-plastic analysis of thick-walled spherical pressure vessels made of functionally graded materials, *International Journal of Applied Mechanics*, Vol. 8, No. 4, pp. 1650054, 2016.
- [5] M. Z. Nejad, M. D. Kashkoli, Time-dependent thermo-creep analysis of rotating FGM thick-walled cylindrical pressure vessels under heat flux, *International Journal of Engineering Science*, Vol. 82, pp. 222-237, 2014.
- [6] A. R. Shahani, F. Kiarasi, Numerical and experimental investigation on post-buckling behavior of stiffened cylindrical shells with cutout subject to uniform axial compression, *Journal of Applied and Computational Mechanics*, Vol. 9, No. 1, pp. 25-44, 2023.
- [7] M. Z. Nejad, N. Alamzadeh, A. Hadi, Thermoelastoplastic analysis of FGM rotating thick cylindrical pressure vessels in linear elastic-fully plastic condition, *Composites Part B-Engineering*, Vol. 154, pp. 410-422, 2018.
- [8] T. Taghizadeh, M. Z. Nejad, M. D. Kashkoli, Thermo-elastic creep analysis and life assessment of thick truncated conical shells with variable thickness, *International Journal of Applied Mechanics*, Vol. 11, No. 9, pp. 1950086, 2019.
- [9] A. Farajpour, A. Rastgoo, Size-dependent static stability of magneto-electro-elastic CNT/MT-based composite nanoshells under external electric and magnetic fields, *Microsystem Technologies*, Vol. 23, pp. 5815-5832, 2017.

- [10] M. D. Kashkoli, K. N. Tahan, M. Z. Nejad, Creep damage and life assessment of thick cylindrical pressure vessels with variable thickness made of 304L austenitic stainless steel, *Steel and Composite Structures*, Vol. 32, No. 6, pp. 701, 2019.
- [11] M. Z. Nejad, T. Taghizadeh, S. J. Mehrabadi, S. Herasati, Elastic analysis of carbon nanotube-reinforced composite plates with piezoelectric layers using shear deformation theory, *International Journal of Applied Mechanics*, Vol. 9, No. 1, pp. 1750011, 2017.
- [12] T. Ebrahimi, M. Z. Nejad, H. Jahankohan, A. Hadi, Thermoelastoplastic response of FGM linearly hardening rotating thick cylindrical pressure vessels, *Steel and Composite Structures*, Vol. 38, No. 2, pp. 189-211, 2021.
- [13] M. D. Kashkoli, K. N. Tahan, M. Z. Nejad, Time-dependent thermomechanical creep behavior of FGM thick hollow cylindrical shells under non-uniform internal pressure, *International Journal of Applied Mechanics*, Vol. 9, No. 6, pp. 1750086, 2017.
- [14] M. H. Dindarloo, L. Li, Vibration analysis of carbon nanotubes reinforced isotropic doubly-curved nanoshells using nonlocal elasticity theory based on a new higher order shear deformation theory, *Composites Part B-Engineering*, Vol. 175, pp. 107170, 2019.
- [15] N. K. Lamba, Impact of memory-dependent response of a thermoelastic thick solid cylinder, *Journal of Applied and Computational Mechanics*, Vol. 9, No. 4, pp. 1135-1143, 2023.
- [16] M. Dehghan, M. Z. Nejad, A. Moosaie, Thermo-electro-elastic analysis of functionally graded piezoelectric shells of revolution: Governing equations and solutions for some simple cases, *International Journal of Engineering Science*, Vol. 104, pp. 34-61, 2016.
- [17] M. Z. Nejad, P. Fatehi, Exact elasto-plastic analysis of rotating thick-walled cylindrical pressure vessels made of functionally graded materials, *International Journal of Engineering Science*, Vol. 86, pp. 26-43, 2015.
- [18] M. Kashkoli, K. N. Tahan, M. Nejad, Time-dependent creep analysis for life assessment of cylindrical vessels using first order shear deformation theory, *Journal of Mechanics*, Vol. 33, No. 4, pp. 461-474, 2017.
- [19] A. Amiri Delouei, A. Emamian, S. Karimnejad, Y. Li, An exact analytical solution for heat conduction in a functionally graded conical shell, *Journal of Applied and Computational Mechanics*, Vol. 9, No. 2, pp. 302-317, 2023.
- [20] A. Sofiyev, N. Fantuzzi, Analytical solution of stability and vibration problem of clamped cylindrical shells containing functionally graded layers within shear deformation theory, *Alexandria Engineering Journal*, Vol. 64, pp. 141-154, 2023.
- [21] M. Nejad, Z. Hoseini, A. Niknejad, M. Ghannad, Steady-state creep deformations and stresses in FGM rotating thick cylindrical pressure vessels, *Journal of Mechanics*, Vol. 31, No. 1, pp. 1-6, 2015.
- [22] Y.-W. Zhang, G.-L. She, Nonlinear primary resonance of axially moving functionally graded cylindrical shells in thermal environment, *Mechanics of Advanced Materials and Structures*, pp. 1-13, 2023.
- [23] C. Ipek, Vibration analysis of shear deformable cylindrical shells made of heterogeneous anisotropic material with clamped edges, *Journal of Applied and Computational Mechanics*, Vol. 9, No. 3, pp. 861-869, 2023.
- [24] M. D. Kashkoli, M. Z. Nejad, Time-dependent creep analysis and life assessment of 304 L austenitic stainless steel thick pressurized truncated conical shells, *Steel and Composite Structures*, Vol. 28, No. 3, pp. 349-362, 2018.
- [25] M. D. Kashkoli, M. Z. Nejad, Time-dependent thermo-elastic creep analysis of thick-walled spherical pressure vessels made of functionally graded materials, *Journal of Theoretical and applied Mechanics*, Vol. 53, No. 4, pp. 1053-1065, 2015.
- [26] I. Panferov, Stresses in a transversely isotropic conical elastic pipe of constant thickness under a thermal load, *Journal of Applied Mathematics and Mechanics*, Vol. 56, No. 3, pp. 410-415, 1992.
- [27] H. Xiang, Z. Shi, T. Zhang, Elastic analyses of heterogeneous hollow cylinders, *Mechanics Research Communications*, Vol. 33, No. 5, pp. 681-691, 2006.
- [28] M. Arefi, G. H. Rahimi, Thermo elastic analysis of a functionally graded cylinder under internal pressure using first order shear deformation theory, *Scientific Research and Essays*, Vol. 5, No. 12, pp. 1442-1454, 2010.
- [29] M. Z. Nejad, G. H. Rahimi, Deformations and stresses in rotating FGM pressurized thick hollow cylinder under thermal load, *Scientific Research and Essays*, Vol. 4, No. 3, pp. 131-140, 2009.
- [30] L. Xin, G. Dui, S. Yang, D. Zhou, Solutions for behavior of a functionally graded thick-walled tube subjected to mechanical and thermal loads, *International Journal of Mechanical Sciences*, Vol. 98, pp. 70-79, 2015.
- [31] M. Z. Nejad, G. H. Rahimi, M. Ghannad, Set of field equations for thick shell of revolution made of functionally graded materials in curvilinear coordinate system, *Mechanika*, Vol. 77, No. 3, pp. 18-26, 2009.
- [32] A. Yasinsky, L. Tokova, Inverse problem on the identification of temperature and thermal stresses in an FGM hollow cylinder by the surface displacements, *Journal of Thermal Stresses*, Vol. 40, No. 12, pp. 1471-1483, 2017.

- [33] M. Ghannad, M. Z. Nejad, Elastic analysis of pressurized thick hollow cylindrical shells with clamped-clamped ends, *Mechanika*, Vol. 85, No. 5, pp. 11-18, 2010.
- [34] J.-H. Kang, Field equations, equations of motion, and energy functionals for thick shells of revolution with arbitrary curvature and variable thickness from a three-dimensional theory, *Acta Mechanica*, Vol. 188, No. 1-2, pp. 21-37, 2007.
- [35] M. Z. Nejad, M. Jabbari, M. Ghannad, A semi-analytical solution of thick truncated cones using matched asymptotic method and disk form multilayers, *Archive of Mechanical Engineering*, Vol. 61, No. 3, pp. 495-513, 2014.
- [36] M. Ghannad, G. H. Rahimi, M. Z. Nejad, Determination of displacements and stresses in pressurized thick cylindrical shells with variable thickness using perturbation technique, *Mechanika*, Vol. 18, No. 1, pp. 14-21, 2012.
- [37] B. Sundarasivarao, N. Ganesan, Deformation of varying thickness of conical shells subjected to axisymmetric loading with various end conditions, *Engineering Fracture Mechanics*, Vol. 39, No. 6, pp. 1003-1010, 1991.
- [38] I. Mirsky, G. Herrmann, Axially symmetric motions of thick cylindrical shells, 1958.
- [39] F. Witt, Thermal stress analysis of conical shells, *Nuclear Structural Engineering*, Vol. 1, No. 5, pp. 449-456, 1965.
- [40] H. R. Eipakchi, S. Khadem, G. H. Rahimi S, Axisymmetric stress analysis of a thick conical shell with varying thickness under nonuniform internal pressure, *Journal of Engineering Mechanics*, Vol. 134, No. 8, pp. 601-610, 2008.
- [41] M. Ghannad, M. Z. Nejad, Elastic solution of pressurized clamped-clamped thick cylindrical shells made of functionally graded materials, *Journal of Theoretical and Applied Mechanics*, Vol. 51, No. 4, pp. 1067-1079, 2013.
- [42] K. Jane, Y. Wu, A generalized thermoelasticity problem of multilayered conical shells, *International Journal of Solids and Structures*, Vol. 41, No. 9-10, pp. 2205-2233, 2004.
- [43] M. Ghannad, M. Z. Nejad, G. H. Rahimi, Elastic solution of axisymmetric thick truncated conical shells based on first-order shear deformation theory, *Mechanika*, Vol. 79, No. 5, pp. 13-20, 2009.
- [44] Y. Obata, N. Noda, Steady thermal stresses in a hollow circular cylinder and a hollow sphere of a functionally gradient material, *Journal of Thermal Stresses*, Vol. 17, No. 3, pp. 471-487, 1994.
- [45] M. Ghannad, G. H. Rahimi, M. Z. Nejad, Elastic analysis of pressurized thick cylindrical shells with variable thickness made of functionally graded materials, *Composites Part B-Engineering*, Vol. 45, No. 1, pp. 388-396, 2013.
- [46] H. R. Eipakchi, Third-order shear deformation theory for stress analysis of a thick conical shell under pressure, *Journal of Mechanics of Materials and Structures*, Vol. 5, No. 1, pp. 1-17, 2010.
- [47] G. Cao, Z. Chen, L. Yang, H. Fan, F. Zhou, Analytical study on the buckling of cylindrical shells with arbitrary thickness imperfections under axial compression, *Journal of Pressure Vessel Technology*, Vol. 137, No. 1, pp. 011201, 2015.
- [48] M. Z. Nejad, M. Jabbari, M. Ghannad, Elastic analysis of axially functionally graded rotating thick cylinder with variable thickness under non-uniform arbitrarily pressure loading, *International Journal of Engineering Science*, Vol. 89, pp. 86-99, 2015.
- [49] Ö. Civalek, Vibration analysis of laminated composite conical shells by the method of discrete singular convolution based on the shear deformation theory, *Composites Part B-Engineering*, Vol. 45, No. 1, pp. 1001-1009, 2013.
- [50] M. Z. Nejad, M. Jabbari, M. Ghannad, Elastic analysis of rotating thick cylindrical pressure vessels under non-uniform pressure: linear and non-linear thickness, *Periodica Polytechnica Mechanical Engineering*, Vol. 59, No. 2, pp. 65-73, 2015.
- [51] S. Ray, A. Loukou, D. Trimis, Evaluation of heat conduction through truncated conical shells, *International Journal of Thermal Sciences*, Vol. 57, pp. 183-191, 2012.
- [52] M. Z. Nejad, M. Jabbari, M. Ghannad, Elastic analysis of FGM rotating thick truncated conical shells with axially-varying properties under non-uniform pressure loading, *Composite Structures*, Vol. 122, pp. 561-569, 2015.
- [53] M. Jabbari, M. Z. Nejad, M. Ghannad, Thermoelastic analysis of rotating thick truncated conical shells subjected to non-uniform pressure, *Journal of Solid Mechanics*, Vol. 8, No. 3, pp. 466-481, 2016 .
- [54] M. Jabbari, M. Z. Nejad, M. Ghannad, Stress analysis of rotating thick truncated conical shells with variable thickness under mechanical and thermal loads, *Journal of Solid Mechanics*, Vol. 9, No. 1, pp. 100-114, 2017.
- [55] A. A. Hamzah, H. K. Jobair, O. I. Abdullah, E. T. Hashim, L. A. Sabri, An investigation of dynamic behavior of the cylindrical shells under thermal effect, *Case Studies in Thermal Engineering*, Vol. 12, pp. 537-545, 2018.

- [56] M. D. Kashkoli, K. N. Tahan, M. Z. Nejad, Thermomechanical creep analysis of FGM thick cylindrical pressure vessels with variable thickness, *International Journal of Applied Mechanics*, Vol. 10, No. 1, pp. 1850008, 2018.
- [57] H. Gharooni, M. Ghannad, M. Z. Nejad, Thermo-elastic analysis of clamped-clamped thick FGM cylinders by using third-order shear deformation theory, *Latin American Journal of Solids and Structures*, Vol. 13, pp. 750-774, 2016.
- [58] M. Jabbari, M. Z. Nejad, M. Ghannad, Thermo-elastic analysis of axially functionally graded rotating thick truncated conical shells with varying thickness, *Composites Part B-Engineering*, Vol. 96, pp. 20-34, 2016.
- [59] J. Lai, C. Guo, J. Qiu, H. Fan, Static analytical approach of moderately thick cylindrical ribbed shells based on first-order shear deformation theory, *Mathematical Problems in Engineering*, Vol. 2015, 2015.
- [60] M. Z. Nejad, M. Jabbari, M. Ghannad, A general disk form formulation for thermo-elastic analysis of functionally graded thick shells of revolution with arbitrary curvature and variable thickness, *Acta Mechanica*, Vol. 228, pp. 215-231, 2017.
- [61] F. Aghaienezhad, R. Ansari, M. Darvizeh, On the stability of hyperelastic spherical and cylindrical shells subjected to external pressure using a numerical approach, *International Journal of Applied Mechanics*, Vol. 14, No. 10, pp. 2250094, 2022.
- [62] O. Ifayefunmi, D. Ruan, Buckling of stiffened cone-cylinder structures under axial compression, *International Journal of Applied Mechanics*, Vol. 14, No. 7, pp. 2250075, 2022.
- [63] M. Y. Ariatapeh, M. Shariyat, M. Khosravi, Semi-analytical large deformation and three-dimensional stress analyses of pressurized finite-length thick-walled incompressible hyperelastic cylinders and pipes, *International Journal of Applied Mechanics*, Vol. 15, No. 1, pp. 2250100, 2023.
- [64] S. Mannani, L. Collini, M. Arefi, Mechanical stress and deformation analyses of pressurized cylindrical shells based on a higher-order modeling, *Defence Technology*, Vol. 20, pp. 24-33, 2023.
- [65] M. Ghannad, M. P. Yaghoobi, 2D thermo elastic behavior of a FG cylinder under thermomechanical loads using a first order temperature theory, *International Journal of Pressure Vessels and Piping*, Vol. 149, pp. 75-92, 2017.
- [66] S. Vlachoutsis, Shear correction factors for plates and shells, *International Journal for Numerical Methods in Engineering*, Vol. 33, No. 7, pp. 1537-1552, 1992.